Probing Cu doped $Ge_{0.3}Se_{0.7}$ based resistance switching memory devices with random telegraph noise

R. Soni, P. Meuffels, A. Petraru, M. Weides, C. Kügeler, R. Waser, and H. Kohlstedt

Citation: Journal of Applied Physics **107**, 024517 (2010);
View online: https://doi.org/10.1063/1.3291132
View Table of Contents: http://aip.scitation.org/toc/jap/107/2
Published by the American Institute of Physics

Articles you may be interested in

Resistance-dependent amplitude of random telegraph-signal noise in resistive switching memories
Applied Physics Letters **96**, 053503 (2010); 10.1063/1.3304167

On the stochastic nature of resistive switching in Cu doped $Ge_{0.3}Se_{0.7}$ based memory devices
Journal of Applied Physics **110**, 054509 (2011); 10.1063/1.3631013

Electrode dependence of filament formation in HfO_2 resistive-switching memory
Journal of Applied Physics **109**, 084104 (2011); 10.1063/1.3567915

Enhancement of resistive switching properties in nitride based CBRAM device by inserting an Al_2O_3 thin layer
Applied Physics Letters **110**, 203102 (2017); 10.1063/1.4983465

Rate limiting step for the switching kinetics in Cu doped $Ge_{0.3}Se_{0.7}$ based memory devices with symmetrical and asymmetrical electrodes
Journal of Applied Physics **113**, 124504 (2013); 10.1063/1.4797488

Field-induced resistive switching in metal-oxide interfaces
Applied Physics Letters **85**, 317 (2004); 10.1063/1.1768305

Probing Cu doped $Ge_{0.3}Se_{0.7}$ based resistance switching memory devices with random telegraph noise

R. Soni,[1,a)] P. Meuffels,[1,a)] A. Petraru,[2] M. Weides,[3] C. Kügeler,[1] R. Waser,[1] and H. Kohlstedt[2,a)]
[1]*Institut für Festkörperforschung, Forschungszentrum Jülich GmbH, Jülich 52425, Germany*
[2]*Nanoelektronik, Technische Fakultät Kiel, Christian-Albrechts-Universität Kiel, Kiel 24143, Germany*
[3]*Department of Physics, University of California, Santa Barbara, California 93106, USA*

(Received 28 October 2009; accepted 14 December 2009; published online 27 January 2010)

The ultimate sensitivity of any solid state device is limited by fluctuations. Fluctuations are manifestations of the thermal motion of matter and the discreteness of its structure which are also inherent ingredients during the resistive switching process of resistance random access memory (RRAM) devices. In quest for the role of fluctuations in different memory states and to develop resistive switching based nonvolatile memory devices, here we present our study on random telegraph noise (RTN) resistance fluctuations in Cu doped $Ge_{0.3}Se_{0.7}$ based RRAM cells. The influence of temperature and electric field on the RTN fluctuations is studied on different resistance states of the memory cells to reveal the dynamics of the underlying fluctuators. Our analysis indicates that the observed fluctuations could arise from thermally activated transpositions of Cu ions inside ionic or redox "double-site traps" triggering fluctuations in the current transport through a filamentary conducting path. Giant RTN fluctuations characterized by relative resistance variations of up to 50% in almost macroscopic samples clearly point to the existence of weak links with small effective cross-sectional areas along the conducting paths. Such large resistance fluctuations can be an important issue for the industrial applications of RRAM devices because they might lead to huge bit-error rates during reading cycles. © *2010 American Institute of Physics*.
[doi:10.1063/1.3291132]

I. INTRODUCTION

Resistive switching phenomena induced by electrical stimulus have been studied since the 1960s, and an enormous range of materials in metal-insulator-metal (MIM) configurations has been reported to show hysteretic resistance switching behavior.[1–15] Recently, the resistance switching based nonvolatile memory device concept, commonly known as resistance random access memory (RRAM), has again evoked great interest within the scientific community as a potential candidate for nonvolatile random access memories and crossbar logic concepts. Attractive properties of RRAMs are low fabrication costs, scalability into the nanometer regime, fast write and read access, low power consumption, and low threshold voltages. Nonetheless, the launching of RRAMs in the market is hindered by several severe obstacles. For example, the microscopic switching mechanism of RRAM devices is still under debate and various models have been proposed to explain the observed phenomena.[12,13,15] By missing a deep understanding of the resistive switching effect on an atomistic scale, a reliable fabrication of Gbit memory circuits with high retention seems to be questionable. On the other hand, in recent years continuous scientific and technological efforts shed more light on the basic ingredients of the resistive switching effect and led to more reliable devices.

There seems to be agreement that lattice defects play a key role with regard to resistive switching mechanisms.[15] These lattice defects are created and/or redistributed within the materials during the so-called electroforming process (a "soft" breakdown) which drives the initially insulating materials into a conducting state. Most of the models are based upon the assumption that these lattice defects form percolating filament-like defect structures within the bulk which locally modify the bulk conductivity of the insulator and/or agglomerate close to an interface of the MIM structure therefore locally modifying the electronic current injection mechanism. Resistance switching memory operation should be possible if the distribution and/or the charge state of these lattice defects can be altered by applying a pulse-like electrical stimulus. It is thus quite obvious that defects play an important role for the characteristic features of such memory devices and that the role of individual defects can become immense in case of filamentary switching processes as one is dealing with defect structures of nanometer-sized dimensions.

In the last few decades, it has been understood that electronic noise which is generated by all materials that constitute electronic devices is not always a nuisance but can also be viewed as a fingerprint of the internal dynamics of defects in devices, reflecting to some extent the material and interface properties on an atomistic scale.[16] In this context, the initial idea for the present work is straightforward. By correlating the noise properties in RRAM devices in dependency on the applied bias voltage, from different resistance states and temperature, the obtained results might be an additional

[a)]Authors to whom correspondence should be addressed. Electronic addresses: r.soni@fz-juelich.de, p.meuffels@fz-juelich.de, and hko@tf.uni-kiel.de.

 © 2010 American Institute of Physics

step on the way to complete the puzzle of resistive switching. Therefore, noise experiments present an attractive tool to gather, so far unknown information, on the atomistic scale for a fully functional RRAM device.

There are three most common types of electronic noise known to exist in materials: Thermal noise which is an intrinsic property of a material and defines the ultimate noise limit, $1/f$ noise at low frequencies which is commonly known as flicker noise and random telegraph noise (RTN). RTN crops up as discrete fluctuations in the current-/voltage-time traces whenever the charge transport through a solid-state device is controlled by the statistical capture/emission of electrons at electron trap sites or the statistical transposition of single lattice defects. Large resistance fluctuations can occur in case the current transport through the device is restricted to current-carrying filamentary paths as these are more affected by microscopic disturbances on an atomistic scale. RTN is characterized by a strong sample-to-sample randomness with regard to the amplitude and rate of the fluctuations and has been observed in a variety of systems:[17] *p-n* junctions,[18] MIM junctions,[19,20] metal oxide semiconductor field effect transistors,[17] and small metallic samples.[21]

Electron trapping/detrapping or the transposition of lattice defects can be influenced by the temperature and the applied electric field. Thus, one can get information about the dynamics of certain "fluctuators" by measuring the average lifetimes, τ_{up} and τ_{down}, during which the sample remains in its "up" state with a higher resistance value, R_{up}, and in its "down" state with a lower resistance value, R_{down}, respectively. The RTN amplitude itself is an important parameter from a reliability point of view. For nanoscaled RRAM devices with a filamentary-type of resistive switching mechanism, such studies become increasingly important—especially, if one aims at multilevel storage application in individual RRAM cells—as RTN can lead to anomalously large relative signal fluctuations. Knowledge on RTN signals in these memory devices seems thus to be necessary prior to industrial qualification.

In the present study, RTN in Cu doped $Ge_{0.3}Se_{0.7}$ based resistance switching memory devices is investigated. In case of ion conducting chalcogenide-based solid electrolytes (SEs), the switching mechanism falls into the category of filamentary nature.[22,23] Mitkova *et al.*[24] have shown that the dissolution of Ag in Se-rich Ge_xSe_{1-x} produces a ternary that is a combination of a separate dispersed mixed ionic-electronic conducting Ag_2Se phase and a continuous high-resistivity Ge-rich Ge–Se backbone phase. We assume that the present system-Cu doped $Ge_{0.3}Se_{0.7}$-behaves in a similar manner because both doped glasses seem to possess comparable properties.[25] The ternary system is superionic at room temperature thus allowing the fast transport of metal ions (M=Ag,Cu). Under an applied positive bias to an oxidizable M electrode, metal ions migrate by a coordinated process toward the cathode where metal electrodeposition starts. In course of this process, metal clusters bridge the high-resistivity glassy regions (Ge–Se-backbone) between the mixed ionic-electronic conducting metal-rich phases (M_2Se) so that finally a conduction path (or a filament) for the electronic transport is established between the anode and the cathode. It is thus justified to speak of the "biased percolation" of a filamentary conducting structure inside a metal-insulator composite. The memory cell instantaneously switches to a low resistance, "ON" state. With the reversal of the bias voltage polarity, the "short-cutting" filaments break at the weakest point due to electrochemical dissolution of the metal atoms and the memory cell switches back to the high resistance, "OFF" state.

II. EXPERIMENTAL

The memory cells were fabricated as cross-point structures with $Ge_{0.3}Se_{0.7}$ active layers and with areas ranging from 2 to 150 μm^2. Si (100) wafers with a 400 nm thermal oxide and a 5 nm TiO_2 film as an adhesion layer for the Pt base electrode deposition were used as substrates. A 30 nm thin film of Pt was sputtered on top. The bottom Pt electrode was patterned by standard optical lithography and by reactive ion beam etching (RIBE). The photoresist was removed with acetone and a buffer layer of 2–3 nm SiO_x was deposited by radio frequency (rf) sputtering at a rate of 0.8 nm s^{-1} followed by defining the bottom electrode contact with optical lithography and RIBE. Afterwards, the orthogonal top structure of the cross-bar was defined by a lift-off step. $Ge_{0.3}Se_{0.7}$ layers with thicknesses 60–70 nm were deposited by rf-sputtering followed by the deposition of the 100 nm Cu top electrode. The deposition rates for the $Ge_{0.3}Se_{0.7}$ and Cu layers were around 0.2 and 0.5 nm s^{-1}, respectively. Finally, a lift-off in acetone was used to finalize the device.

An Agilent B1500 semiconductor parameter analyzer was employed for two point quasistatic current-voltage measurements. RTN measurements were performed using a battery-powered low noise current source and an HP 35670A spectrum analyzer. A constant current was applied to the memory cells and the spectrum analyzer was used to record the RTN signals. Low temperature measurements were performed in a continuous flow cryostat. Considerable efforts were put for proper shielding to minimize 50 Hz and rf pickup noises.

III. RESULTS AND DISCUSSION

A. RTN experiments

The characteristics of RTN were analyzed for different resistance states of Cu doped $Ge_{0.3}Se_{0.7}$ based memory devices as a function of temperature and current flow through the devices. A schematic of a single cross-point structure is shown in Fig. 1(a). A very thin SiO_x diffusion barrier was introduced between the Cu–Ge–Se layer and the Pt bottom electrode to improve the switching characteristics[26] and to achieve very low leakage currents. Starting from the OFF state of the devices, the different resistance states were adjusted by programming the memory cells with quasistatic current-voltage (I-V) sweeps using appropriate settings of the current compliance as shown in Fig. 1(b). More details on the memory device properties such as retention, endurance, nanoampere switching, and reliability can be found in Refs. 26 and 27.

The RTN signals of our memory devices were very sensitive to the current flow through the samples and to the

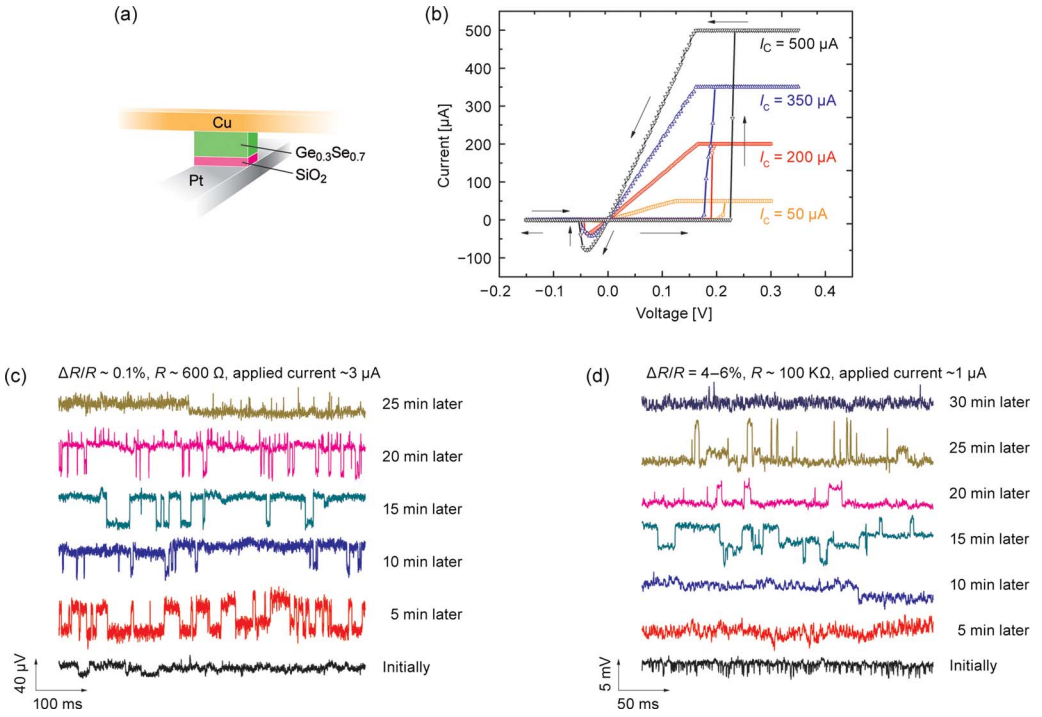

FIG. 1. (Color online) (a) Schematic of a Cu doped $Ge_{0.3}Se_{0.7}$ based memory cell. (b) Room temperature *I-V* characteristics of a memory cell programmed by using different settings of the current compliance I_c. (c) Time records of unstable RTN fluctuations measured at 300 K under an applied current of 3 μA on a memory cell in a LRS of ≈600 Ω. (d) Time records of unstable RTN fluctuations measured at 300 K under an applied current of 1 μA on a memory cell in a HRS of ≈100 kΩ.

temperature so that these external parameters had to be selected in an appropriate range. It was particularly difficult to observe stable RTN at room temperature in case a very low current (typically <3 μA) was applied to memory devices which were programmed to lower resistance states (LRS) with resistance values <5 kΩ. Figure 1(c) illustrates the unstable nature of the fluctuations under these conditions. At higher currents (typically >20 μA), RTN could be easily observed. In case of devices that were programmed to higher resistance states (HRS) with resistance values >80 kΩ, it was comparatively easy to observe RTN at low applied currents (typically at 1 μA) at room temperature. Frequently, however, the fluctuations in the voltage-time traces disappeared or came and went repeatedly with a given waveform rarely persisting without change from more than a few traces as shown, for example, in Fig. 1(d). With decreasing temperature, very stable RTN signals were usually found between 150 and 270 K. However, the signals appeared randomly at a certain temperature which was unique for every device. When stable RTN could be observed on our memory devices, it stayed for about 5–10 h so that we were able to analyze the current (or voltage) and temperature dependence of the signal characteristics.

All samples displayed discrete RTN resistance fluctuations with relative variations, $\Delta R/R=(R_{up}-R_{down})/R_{up}$, ranging from 0.1% up to 12%, depending on the given resistances to which the memory devices had been programmed. As the observed resistance fluctuations were quite large, the dependence of the average fluctuator lifetimes, τ_{up} and τ_{down}, on the applied current and temperature could be mapped out with high precision thus allowing us to gain some access to the microscopic properties of the underlying fluctuators. In our experiments, the accessible time window ranged from 15 msec to 1 min. In case the average lifetimes of an active fluctuator lie outside the experimental window, RTN cannot be observed directly.

The average lifetimes can be derived by means of a statistical analysis of the time spans the active fluctuator spends in its up and down state. The individual transition probabilities P_{up} and P_{down} are expected to be distributed exponentially by[17]

$$P_{up,down}(t) \propto \exp(-t/\tau_{up,down}). \quad (1)$$

Here, P_{up} refers to the probability per unit time that the RTN fluctuator stays in its up state for a certain time span t and then switches to the down state. The reverse holds for P_{down}. By fitting the time distributions with this function, both τ_{up} and τ_{down} could be extracted from the recorded data.

Figure 2(a) shows as an example a stable waveform trace of RTN observed at 240 K on a memory cell which was initially programmed to a resistance of ≈3 kΩ. The measurements were performed under an applied constant current of 40 μA. The resulting voltage noise spectral power density $S_V(f)$ can be seen in Fig. 2(b). The relative resistance variation, $\Delta R/R$, was found to be approximately 5% corresponding to a voltage fluctuation amplitude of $\delta V \approx 6$ mV. Figure 2(c) shows the time distributions for the up and down states of the observed RTN fluctuator. Using Eq. (1) to fit the experimental data, we obtained $\tau_{up} \approx 0.3$ ms and $\tau_{down} \approx 1.6$ ms for this particular case.

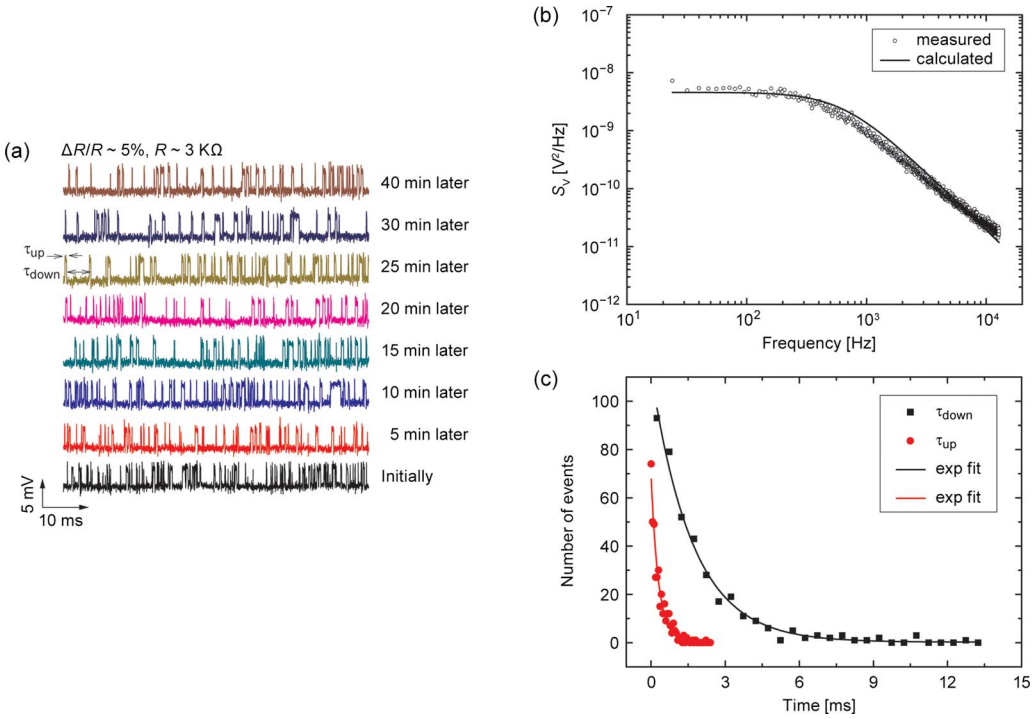

FIG. 2. (Color online) (a) Time records of stable RTN fluctuations measured at 240 K under an applied current of 40 μA on a memory cell in a LRS of $\approx$3 kΩ. (b) Measured (open symbols) and calculated (straight line) voltage noise spectral power density $S_V(f)$ for the memory cell with the two level RTN shown in (a). (c) Histograms of the up and down times for the RTN signal showing that the times in both states follow an exponential distribution.

Machlup[28] calculated the voltage noise spectral power density $S_V(\omega)$ from a two level random signal and derived the following equations:

$$S_V(\omega) = 4(\delta V^2)[\tau_{\text{eff}}/(\tau_{\text{up}} + \tau_{\text{down}})][\tau_{\text{eff}}/(1 + \omega^2 \tau_{\text{eff}}^2)], \quad (2a)$$

$$1/\tau_{\text{eff}} = 1/\tau_{\text{up}} + 1/\tau_{\text{down}}. \quad (2b)$$

Here, $\omega = 2\pi f$ is the angular frequency and δV the amplitude of the voltage fluctuations. Inserting the obtained values for τ_{up}, τ_{down}, and δV, we found that these equations provide an excellent quantitative connection between the real time behavior [Fig. 2(a)] and the measured $S_V(f)$ [Fig. 2(b)]. The calculated spectrum is shown as a straight line in Fig. 2(b). It is obvious that the voltage noise spectral power density is indeed largely given by a single Lorentzian contribution to the spectrum. The observed deviations between the measured and calculated spectra at high frequencies might possibly be attributed to ion migration in the material and further $1/f$ noise studies are needed to elucidate these dependencies.

B. Electric field dependence of RTN resistance fluctuations

Our findings of giant RTN signals in Cu doped $Ge_{0.3}Se_{0.7}$ based memory devices remind somehow of the findings made on hydrogenated amorphous silicon (a-Si:H).[29,30] RTN in a-Si:H seems to result from time dependent changes in the conductance of inhomogeneous current paths networking the film that are sensitive to hydrogen motion. Generally, there is strong evidence that defect motions which locally change the effective electron mean free path can be the source of noise in solid materials.[31,32] In view of this, we thus suppose that the distinct resistance fluctuations observed on Cu doped $Ge_{0.3}Se_{0.7}$ based memory devices might be related to the motion of charged defects like Cu ions which interfere with the current transport through the filamentary conducting structure. The current transport reflects the detailed atomistic configuration along this structure. Minor deviations can locally degrade or strengthen the path, especially, when weak links or critical bonds with their reduced "effective cross-sectional area" are affected. A few fluctuators located in or near to such critical bonds could thus have a dramatic effect on the overall connectivity of the conducting path, which can result in a large increase in the noise level.

A standard model used to describe ion migration in disordered solids assumes the existence of a random potential landscape where the ions are randomly distributed over the local minima ("sites"). Ion movement is due to activated transitions over the energy barriers separating these sites.[33] Figure 3(a) schematically shows a one-dimensional representation of the three-dimensional ion hopping model for a Cu doped Ge_xSe_{1-x} based SE. On principle, one has to take into account a free energy landscape since in the present heterogeneous system ion hopping will frequently occur between different phases resulting in electrochemical reactions. In order to simplify the following presentation, this point will be discussed later on.

In case the observed RTN fluctuations result from the transposition of charged defects, the average fluctuator lifetimes should depend on the external applied bias (or applied current flow) as the energy landscape will be deformed by the contribution of the electric potential energy. We have therefore examined how the average lifetimes of an active RTN fluctuator are influenced by the applied current (i.e., potential drop) through a memory cell. Exemplary RTN time

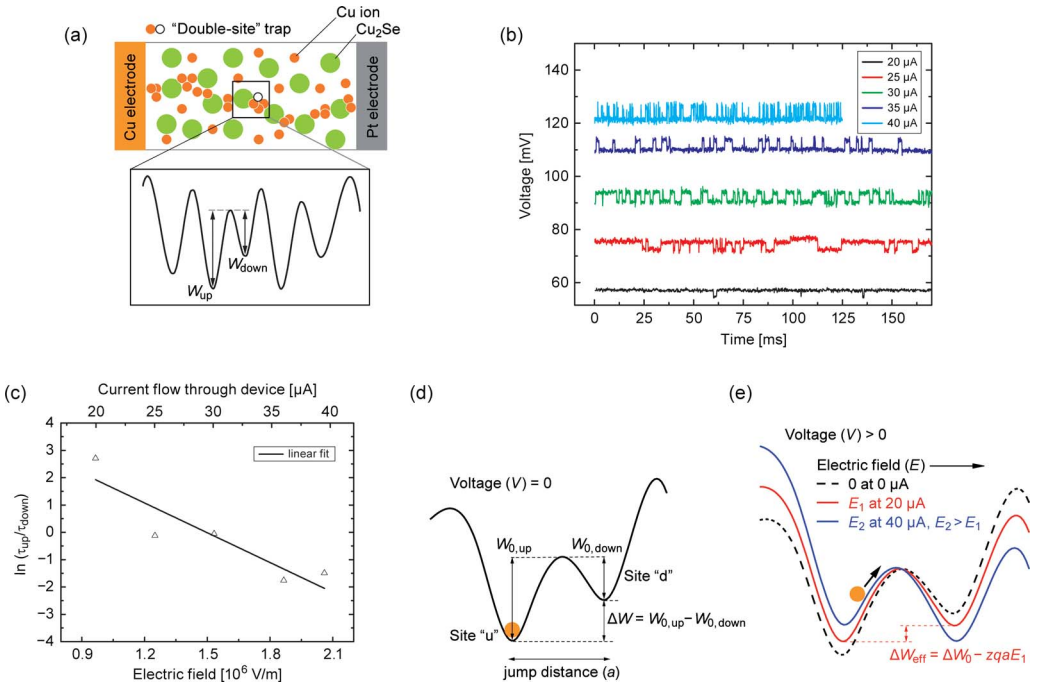

FIG. 3. (Color online) (a) One dimensional representation of the 3D ion hopping model for Cu doped $Ge_{0.3}Se_{0.7}$ SE based memory cells. (b) Time records of stable RTN fluctuations measured at 240 K under varying applied currents (i.e., potential drops) on a memory cell in a LRS of ≈3 kΩ. (c) The ratio of the average lifetimes for the up and down state of the RTN fluctuator as a function of the average applied electric field and current flow through the memory cell. (d)-(e) Schematics of an asymmetric double-well potential for a fluctuating Cu ion without (d) and with (e) an applied electric field showing the deformation of the potential wells under applied bias.

records for this type of measurement are shown in Fig. 3(b). The measurements were performed at 240 K on a device which was initially programmed into a LRS of ≈3 kΩ. As one can see from Fig. 3(b), the time spans the fluctuator spent in its up and down state depended strongly on a small increment in applied current. The relative resistance fluctuations were approximately independent of the current flow, indicating switching of the same fluctuator during these measurements. Interestingly, we found that the ratio between the average lifetimes for the up and down states started to invert with increasing current flow, i.e., the time the fluctuator stayed in its up state at 20 μA was longer than the time it stayed in its down state and vice versa at 40 μA [see Fig. 3(c)].

The observation can be qualitatively understood under the assumption that the fluctuation arises from a Cu ion which hops back and forth between the two sites of a double-site trap which is characterized by an asymmetric double-well potential as schematically depicted in Fig. 3(d). Simulations of the silver dynamics in Ag doped chalcogenide glasses point to the existence of so-called supertraps or cages for silver ions that consist of multiple trapping center sites within a small volume.[34] Long range silver motion proceeds via the hopping between these supertraps. Certainly, the same will as well apply to Cu doped $Ge_{0.3}Se_{0.7}$. In such a highly disordered material, there will be always some regions where two neighboring supertraps are energetically coupled to each other in such a way that a deep ionic double-site trap is formed.

Ion hopping is a thermally activated process, i. e. the Cu^{z+} ion has to surmount a certain energy barrier, $W_{0,up}$ or $W_{0,down}$, in order to jump from site (u) to site (d) or vice versa [see Fig. 3(d)]. The application of an electric field E deforms the potential wells and results in a change of the effective barriers by $\sim -\alpha zqEa$ for the jump (u)→(d) and $\sim +(1-\alpha)zqEa$ for the jump (d)→(u) as illustrated in Fig. 3(e) (α: asymmetry factor for the double-well potential, z: valence number of the ion, q: elementary charge, and a: jump distance). Strictly spoken, one has to consider that the electric field E acting upon a given fluctuator depends on the fluctuator's state itself as fluctuation-induced local changes in the conductivity feed back on the electric field distribution across the whole filamentary conducting path. To simplify, we assume, however, that the acting electric field will be roughly the same for both states. For a given fixed atomistic configuration along a filamentary conducting path, the actual electric field E at a particular location will always exhibit some proportionality to the average applied electric field, V/d (V: applied bias, d: thickness of the Cu doped $Ge_{0.3}Se_{0.7}$ layer), so that we assume as a first approximation $E \approx \beta V/d$.

The transition rates for the transpositions (u)→(d) and (d)→(u) are inversely proportional to the average times the hopping ion stays on trap site (u) and trap site (d), respectively [up state: ion at site (u), down state: ion at site (d)]. According to our fluctuator model, we thus end up with the following equations for the average lifetimes, τ_{up} and τ_{down},

$$1/\tau_{up} = \nu_{app,up} \exp[-(W_{0,up} - \alpha zqa\beta V/d)/k_B T], \tag{3a}$$

$$1/\tau_{down} = \nu_{app,down} \exp\{-[W_{0,down} + (1-\alpha)zqa\beta V/d]/k_B T\}, \tag{3b}$$

where $\nu_{app,up}$ and $\nu_{app,down}$ are the "apparent attempt frequen-

cies" (discussed later) and $W_{0,\mathrm{up}}-\alpha zqa\beta V/d$ and $W_{0,\mathrm{down}}+(1-\alpha)zqa\beta V/d$ the effective activation energies for the jumps, k_B is the Boltzmann constant, and T is the absolute temperature. The ratio between the average lifetimes of the up and down state can now be written as

$$\ln(\tau_{\mathrm{up}}/\tau_{\mathrm{down}}) = \ln(\nu_{\mathrm{app,down}}/\nu_{\mathrm{app,up}}) + \frac{(W_{0,\mathrm{up}} - W_{0,\mathrm{down}})}{k_B T} - \frac{zqa}{k_B T}\beta\frac{V}{d}. \quad (4)$$

Comparable equations will result in case a fluctuating Cu ion experiences a charge transfer in course of the transposition. One can imagine, for example, that a Cu ion jumps from a lattice site in the Ge–Se glassy backbone phase to an adjoining lattice site on the surface of a metal cluster. If both sites are energetically coupled to each other, this could lead to a fluctuating anodic dissolution/cathodic deposition reaction $\mathrm{Cu_{MC}} \Leftrightarrow \mathrm{Cu_{SE}^{z+}} + z\mathrm{e_{MC}^{-}}$ (redox reaction) at the interface between a metallic cluster (or electrode) and the SE, i. e., a—so to speak—redox double-site trap is formed. Such a type of fluctuator can be described in terms of redox reaction kinetics. Contributions of the externally applied bias to local built-in potential gradients are then treated as local overvoltages.

Equation (4) indeed shows that the ratio between τ_{up} and τ_{down} can depend on the applied external field. Under certain circumstances (e. g.: $\nu_{\mathrm{app,up}} \approx \nu_{\mathrm{app,down}}$, $W_{0,\mathrm{up}} > W_{0,\mathrm{down}}$), the model can predict an inversion of the average lifetime ratio with increasing electric field. Despite the fact, that the detailed microscopic nature of the interaction mechanism between the fluctuator and the filamentary conducting path is still an open question, our simple qualitative model gives strong evidence that the observed resistance fluctuations might result from charged defects like Cu ions hopping back and forth between the two sites of deep redox or ionic double-site traps. Defect fluctuations in the close proximity to a sector of a filamentary conducting path will certainly exert some influence: In case of fluctuations in a redox double-site trap, the defect directly interacts with the conducting filament as a fluctuating "building unit," i. e., the Cu ion is attached to the metallic filament and is reduced to a Cu atom and vice versa. If this takes place at a weak link, the Cu atom might bridge two loosely connected conducting branches of the filament whereby large changes in the overall filament resistance could rise up. In case of fluctuations in an ionic double-site trap, the fluctuating defect can indirectly induce some local spatial distortions along the filament due to long range elastic or electrostatic interactions. Such "interactions" could lead to a fluctuating, cooperative rearrangement of the atomistic configuration within the considered sector whereby the local electronic structure and/or the effective electron mean free path and consequently the overall resistance of the conducting path might be altered.

From the intercept of the line in Fig. 3(c) at $E=0$ (no current) one gets an estimate for $\Delta W_0 = W_{0,\mathrm{up}} - W_{0,\mathrm{down}}$ by means of Eq. (4) assuming as a first approximation $\nu_{\mathrm{app,up}} \approx \nu_{\mathrm{app,down}}$. We obtained $\Delta W_0 \approx 0.11$ eV for the considered fluctuator. Hopping distances between supertraps in Ag doped $\mathrm{Ge}_x\mathrm{Se}_{1-x}$ fall into the range 0.15–0.4 nm.[34] Adopting these values as a rough measure for typical jump distances in both types of double-site traps for the present system, the electric field, $\beta V/d$, at the location of the observed fluctuator can be estimated from the slope of the curve in Fig. 3(c) using Eq. (4). We calculated β values in the range 100–250 ($z=2$) pointing to a strong field enhancement at some locations along the conducting path. This is a reasonable outcome since it is well known that in metal-insulator composites even above the percolation threshold there will be always local "bottlenecks" in the conducting paths which funnel the current and are thus characterized by large local voltage drops.[35,36] Active fluctuators which are close to such bottlenecks can give rise to the largest RTN fluctuations. Measurements as those shown in Fig. 3(c) performed on a set of fluctuators could thus serve as a probe to scan the electric field distribution along percolating, filamentary conducting structures.

C. Temperature dependency of RTN resistance fluctuations

We also investigated the temperature dependence of the average lifetimes for the up and down states of some active RTN fluctuators in order to obtain information about the involved activation energies and attempt frequencies. These measurements were done on memory devices in two different resistance states, a LRS of ≈ 1 kΩ and a HRS of ≈ 80 kΩ, under an applied constant current of 60 and 1 μA, respectively. Figures 4(a) and 4(c) depict the temperature dependence of the RTN signals on the basis of some exemplary RTN time records. The curves are offset for clarity. The arrows in the figures show how the temperature was changed during the measurements. The relative resistance variations $\Delta R/R$ in the both resistance states, LRS and HRS, were $\approx 1\%$ and $\approx 5\%$, respectively. As can be seen, the times spent by the fluctuators in their up and down states increase with decreasing temperature.

In course of such temperature-dependent measurements on one fluctuator, occasionally, fluctuations owing to a second active fluctuator appeared in the RTN time records at a certain temperature [see RTN trace at 200 K in Fig. 4(c)]. This happens when the average lifetimes of the up and down states of the second fluctuator start to fall into the experimental time window at this temperature. In case that both fluctuators act independently of each other, it is easy to distinguish between them because of their different average lifetimes.

Figures 4(b) and 4(d) clearly show that the average lifetimes of the observed fluctuators exhibit a thermally activated behavior [see Eqs. (3a) and (3b)]. The effective activation energies, W, (apparent attempt frequencies, ν_{app}) for the up and down states of the fluctuator in the LRS of the memory device (measured at 60 μA) were found to be ≈ 0.53 eV ($\approx 10^{14}$ s^{-1}) and ≈ 0.65 eV ($\approx 10^{16}$ s^{-1}), respectively. Interestingly, $\nu_{\mathrm{app,up}}$ and $\nu_{\mathrm{app,down}}$ differ by a factor of about 100. At a first glance, this might be surprising since the overall phonon spectrum of solids can never be influenced to such an extent by a single fluctuating defect. However, the

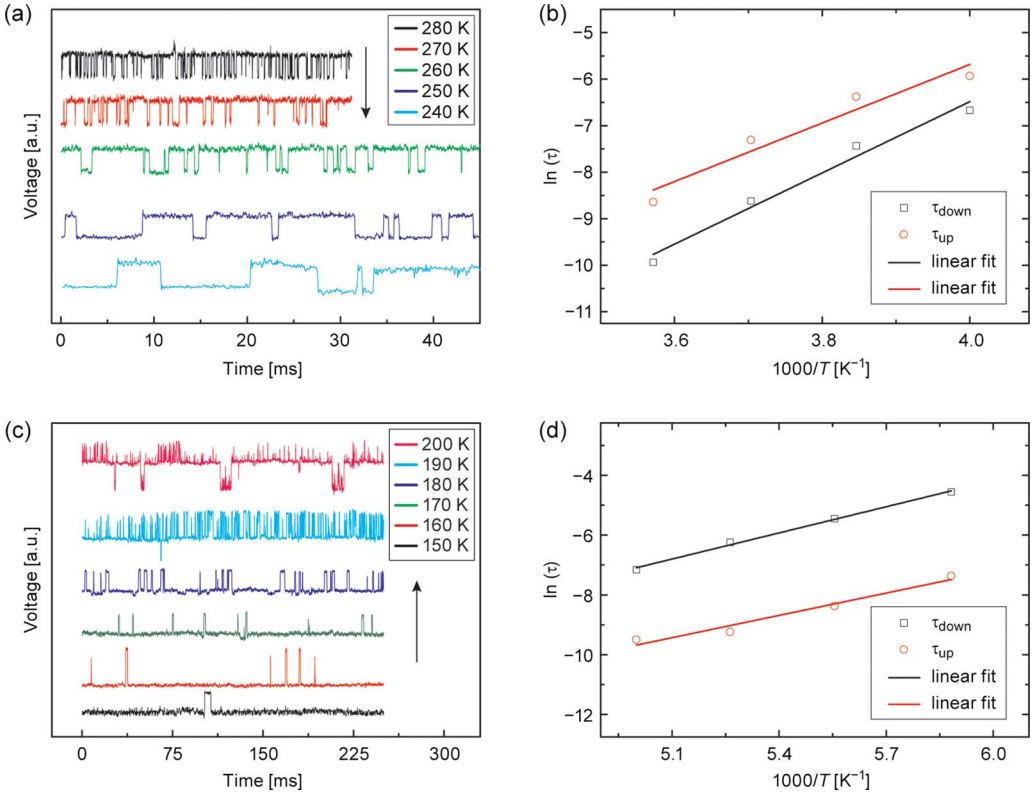

FIG. 4. (Color online) (a) Temperature dependence of the RTN signal of a memory cell in a LRS of ≈1 kΩ. A constant current of 60 μA was flowing through the memory cell during the measurements. (b) Arrhenius plot of the average lifetimes for the up and down states of the RTN fluctuator in the LRS of the device. (c) Temperature dependence of the RTN signal of a memory cell in a HRS of ≈80 kΩ. A constant current of 1 μA was flowing through the memory cell during the measurements. (d) Arrhenius plot of the average lifetimes for the up and down states of the RTN fluctuator in the HRS of the device.

difference can be qualitatively understood if one awakens to the fact that apparent attempt frequencies which are determined from Arrhenius plots like those in Figs. 4(b) and 4(d) contain an entropy related contribution.

It follows from transition-state theory that a defect has to overcome a free energy barrier, $\Delta G = W - T\Delta S$, when jumping from one lattice site to another inside a solid.[37] From the transition rates which are given by

$$1/\tau_{\mathrm{up,down}} = \nu_0 \exp(-\Delta G_{\mathrm{up,down}}/k_B T) = \nu_0 \exp(\Delta S_{\mathrm{up,down}}/k_B)\exp(-W_{\mathrm{up,down}}/k_B T), \quad (5)$$

one arrives at the following expression for the apparent attempt frequencies

$$\nu_{\mathrm{app,(up,down)}} = \nu_0 \exp(\Delta S_{\mathrm{up,down}}/k_B). \quad (6)$$

Here, ν_0 is now the "real attempt frequency" which is correlated with the phonon spectrum. Typical values are of the order 10^{12}–10^{13} s^{-1} which is characteristic of lattice vibrations in solids. $\Delta S_{\mathrm{up,down}}$ is the change in entropy of the system associated with the move of the defect from lattice site (u) (up state) or (d) (down state) to the transition state or saddle point between both sites [refer to Fig. 3(d)].

Weismann[38] has pointed out that entropy related effects have to be considered in case the fluctuation is between different local phases which generally are supposed to have substantially different energies and entropies. Since we are dealing with a very inhomogeneous system, the transposition of Cu ions will frequently occur at the interface between two phases with different entropies, in case of, for example, a "fluctuating redox reaction" as mentioned above. Such a defect fluctuation increases/decreases the number of constituting "building units" for both phases by one unit so that the entropy S of the whole system will alter by a certain amount δS in course of the fluctuation, i.e., $S_{\mathrm{up}} = S_{\mathrm{down}} + \delta S$. When the defect moves to the transition state, the entropy will change by some intermediate amount of both phases.[38] It is reasonable to assume as a first approximation that the entropy S_{ts} of the system in the transition state is independent of the jump direction. A difference in the apparent attempt frequencies for the up and down state of the fluctuator will therefore simply arise because the entropy changes associated with the move of the defect to the transition state differ for both cases, i.e., we have $\Delta S_{\mathrm{up}} = S_{\mathrm{ts}} - S_{\mathrm{up}} \neq \Delta S_{\mathrm{down}} = S_{\mathrm{ts}} - S_{\mathrm{down}}$ and consequently $\nu_{\mathrm{app,up}} \neq \nu_{\mathrm{app,down}}$ [see Eq. (6)].

Let us now consider the high resistive state. Figure 4(d) shows the temperature dependence of the average lifetimes for the up and down states of an active RTN fluctuator in the HRS of a memory device measured at an applied current of 1 μA. In this case, we obtained effective activation energies (apparent attempt frequencies) of ≈0.25 eV (≈10^{10} s^{-1}) and ≈0.22 eV (≈10^{10} s^{-1}) for the down and up state, respectively. As $\nu_{\mathrm{app,up}}$ and $\nu_{\mathrm{app,down}}$ have nearly the same value, the active fluctuator seems to be located—in view of the above discussion—in a homogeneous region inside the ternary glass, presumably in the Ge–Se glassy backbone phase. The obtained values for the effective activation energies are com-

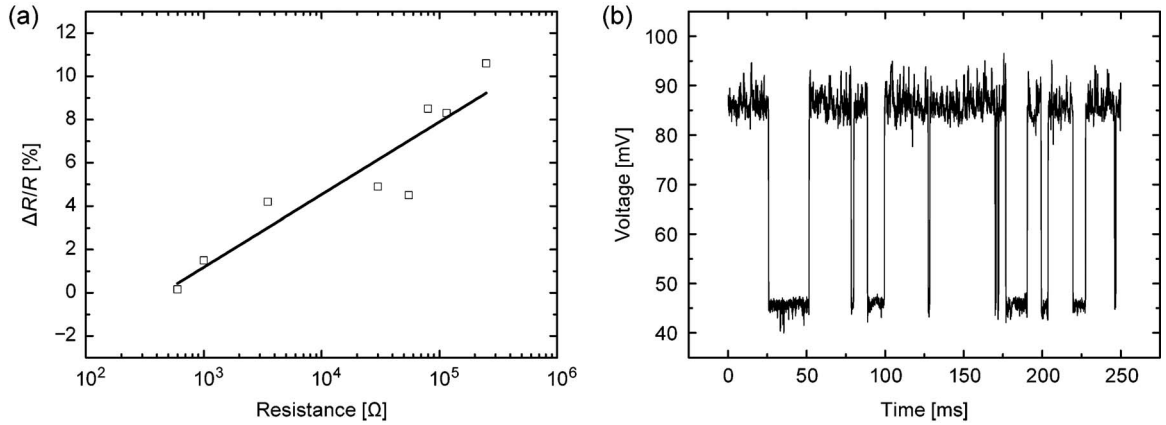

FIG. 5. (a) Typical relative resistance fluctuations, $\Delta R/R$, vs the programmed sample resistance R of Cu doped $Ge_{0.3}Se_{0.7}$ SE based memory cells measured at room temperature under 1 μA current flow. (b) A giant RTN signal with $\Delta R/R \approx 50\%$ observed on a Cu doped $Ge_{0.3}Se_{0.7}$ SE based memory cell in a HRS of ≈ 80 kΩ measured at room temperature under 1 μA current flow.

parable to the low activation energies which are found for metal ion migration in highly metal doped chalcogenide glasses.[39,40] As long range ion migration proceeds via hopping in these disordered ternary compounds, activation energies for hopping are a measure of the mean energy barrier height between two adjacent hopping sites. It is reasonable to assume that the height of these barriers will not change drastically in course that two sites are energetically coupled to form a deep double-site trap. This could be an additional argument that our fluctuator model has some realistic features.

In case of highly disordered material systems, such as metal doped chalcogenides, one generally expects a wide spread of activation energies and "apparent attempt frequencies" for the up and down states of fluctuators which are related to transpositions of charged defects like Cu ions. In the present material system, the atomistic bonding configurations and bonding strengths within the filamentary conducting paths and their surrounding environment certainly depend on the actual degree of percolation so that we furthermore expect that the statistical distribution of the activation energies and apparent attempt frequencies for an assumed double-site trap fluctuator will certainly depend on the resistance state of the memory device. More extensive work is required in future to establish these correlations.

Finally, we would like to emphasize that the temperature-dependent measurements could not simply be repeated as the initial state of the system was never exactly the same after thermal cycling. The RTN signal could vanish altogether or, when present, display different characteristics compared to the foregoing experiment. Similar observations were made on other systems, too.[21,41] This is not surprising as thermally activated atomic movements can alter or passivate any active fluctuator. This indicates the fragile nature of the memory devices with regard to slight disturbances and shows that these inhomogeneous systems can exist in many possible configurations.

D. Amplitude of the RTN resistance fluctuations

The discrete RTN resistance fluctuations which we observed on our samples showed relative large resistance variations, $\Delta R/R$, ranging from 0.1% up to 12%, depending upon the programmed resistance of the memory devices. We typically found that the resistance fluctuations increased with increasing overall resistance of the samples as shown in Fig. 5(a) for memory devices with resistances in the range 600 Ω(LRS)–300 kΩ(HRS). All these measurements were performed with a 1 μA current flow through the devices at room temperature. This interrelation can be understood, at least qualitatively, within the framework of a "classical percolation" model[42] when we regard our inhomogeneous material as a composite material above the percolation threshold.

Percolation is essentially a simple purely geometrical model. The geometrical quantities, such as cluster size distribution, mean size of a finite cluster and correlation length, and the transport properties such as the electrical conductance purely depend on the degree of percolation in the material system and these interconnected physical parameters diverge near the percolation threshold.[42] The overall resistance of our memory cells mirrors the degree of percolation or "percolation strength" in the system, i. e., while going from the "metallic" side (LRS) of the percolating system toward the percolation threshold (HRS), the "strength" of the conducting network and consequently the conductance will decrease. The conducting structure becomes more fragile and therewith more susceptible to disturbances on a microscopic scale. On the average, one would thus expect an increase in the relative resistance fluctuations while going from the LRS to the HRS of the memory devices. Recently, for example, the large $1/f$ noise of unipolar resistance switching devices made of NiO has been related to the percolation process of conducting filaments.[43]

Occasionally, very large RTN signals with $\Delta R/R$ up to 50% were observed on the memory devices as can be seen in Fig. 5(b). The resistance of the device was ≈ 80 kΩ and the measurement was performed at room temperature while applying a current flow of 1 μA. It is important to note that for this resistance state, typically, $\Delta R/R$ values in the range 5%–6% were found, as shown in Fig. 5(a). Generally, for every percolating conducting network at a given degree of percolation there exists an ensemble of different geometrical

structures and critical weak links. Thus, very large resistance fluctuations can arise under those circumstances where an active fluctuator affects one of the weakest connections across the conducting network.

Our results show a close correlation between the programmed resistance state of the devices and the RTN amplitude. The ionic mass transport (here of Cu ions) during the switching process modifies the atomistic structure along the filaments and/or the filament/electrode interfaces. Obviously, these material modifications are inherently coupled to the individual nature of fluctuators which interfere with the current transport through the filamentary conducting structure. Although one might be able to get stable defined resistance states by applying electric stimulus, there always remains the risk that large RTN fluctuations can be present or can suddenly occur. As shown in this study, fluctuations in the voltage amplitude can be significant and cannot be neglected. During data reading cycles, particular for multilevel RRAM cells, these RTN fluctuations would lead to considerable large bit-error rates. In order to avoid that large resistance fluctuations crop up, the creation and disruption of the filamentary conducting structure would have to be accomplished in such a way that fragile and thus disturbance-susceptible connections do preferably not outlive the programming process. This might be a great challenge for RRAM applications owing to the fact that the reorganization of percolating conducting networks in disordered material systems is certainly of stochastic nature.

IV. CONCLUSIONS

To summarize, we have investigated RTN resistance fluctuations for different resistance states of Cu doped $Ge_{0.3}Se_{0.7}$ based resistance switching memory devices. Based upon an analysis of the electric field and temperature dependence, we were able to develop a simple model which relates the observed RTN resistance fluctuations to the thermally activated hopping of Cu ions inside ionic or redox double-site traps which trigger fluctuations in the local conductivity along the filamentary conducting path. The fluctuator properties such as effective activation energies and attempt frequencies seem to depend on the programmed resistance state of the memory devices indicating different atomic bonding configurations along the filamentary conducting structure. The RTN signal amplitude appears to be very sensitive to the resistance state and we identify RTN as a possible failure mechanism for the use of these memory devices in multilevel data storage applications. The preliminary results presented here demonstrate that the study of RTN is a powerful tool to probe local atomistic instabilities which are coupled to fluctuating defects. The fact that the statistical properties of a few defects can have such an enormous influence on the overall conductance of resistance switching memory devices with a filamentary-type of switching mechanism, will certainly be reflected in a large device-to-device randomness with respect to the "set and reset" parameters for resistive switching. We therefore believe that RTN studies on nanoscaled resistance switching memory devices based on other material systems will also be useful to provide information on reliability related issues prior to industrial qualification.

Note added. After submission of this paper we became aware of a recent publication by M. Nardone *et al.*[44] addressing a theoretical analysis of possible mechanisms for $1/f$ noise in chalcogenide glasses. This publication could be very useful for a better understanding of noise in this kind of material systems.

ACKNOWLEDGMENTS

The authors would like to thank K. Szot and T. Menke for helpful discussions and Thomas Pössinger for his assistance in preparing the figures.

[1] T. W. Hickmott, J. Appl. Phys. **33**, 2669 (1962).
[2] J. F. Gibbons and W. E. Beadle, Solid-State Electron. **7**, 785 (1964).
[3] E. L. Cook, J. Appl. Phys. **41**, 551 (1970).
[4] F. A. S. Al-Ramadhan and C. A. Hogarth, J. Mater. Sci. **19**, 1939 (1984).
[5] A. Beck, J. G. Bednorz, Ch. Gerber, C. Rossel, and D. Widmer, Appl. Phys. Lett. **77**, 139 (2000).
[6] C. Rossel, G. I. Meijer, D. Brémaud, and D. Widmer, J. Appl. Phys. **90**, 2892 (2001).
[7] A. Baikalov, Y. Q. Wang, B. Shen, B. Lorenz, S. Tsui, Y. Y. Sun, Y. Y. Xue, and C. W. Chu, Appl. Phys. Lett. **83**, 957 (2003).
[8] K. Szot, W. Speier, G. Bihlmayer, and R. Waser, Nature. Mater. **5**, 312 (2006).
[9] G. Dearnaley, A. M. Stoneham, and D. V. Morgan, Rep. Prog. Phys. **33**, 1129 (1970).
[10] D. P. Oxely, Electrocomponent Sci. Technol. **3**, 217 (1977).
[11] H. Pagnia and N. Sotnik, Phys. Status Solidi A **108**, 11 (1988).
[12] Y. Watanabe, Ferroelectrics **349**, 190 (2007).
[13] R. Waser and M. Aono, Nature. Mater. **6**, 833 (2007).
[14] S. F. Karg, G. I. Meijer, J. G. Bednorz, C. T. Rettner, A. G. Schrott, E. A. Joseph, C. H. Lam, M. Janousch, U. Staub, F. La Mattina, S. F. Alvarado, D. Widmer, R. Stutz, U. Drechsler, and D. Caimi, IBM J. Res. Dev. **52**, 481 (2008).
[15] R. Waser, R. Dittmann, G. Staikov, and K. Szot, Adv. Mater. **21**, 2632 (2009).
[16] S. Kogan, *Electronic Noise and Fluctuations in Solids* (Cambridge University Press, London, UK, 1996).
[17] M. J. Kirton and I. I. Uren, Adv. Phys. **38**, 367 (1989).
[18] D. Wolf and E. Holler, J. Appl. Phys. **38**, 189 (1967).
[19] X. G. Jiang, M. A. Dubson, and J. C. Garland, Phys. Rev. B **42**, 5427 (1990).
[20] H. Kohlstedt, K. H. Gundlach, and S. Kuriki, J. Appl. Phys. **73**, 2564 (1993).
[21] K. S. Ralls and R. A. Buhrman, Phys. Rev. B **44**, 5800 (1991).
[22] M. N. Kozicki, M. Park, and M. Mitkova, IEEE Trans. Nanotechnol. **4**, 331 (2005).
[23] C. Schindler, X. Guo, A. Besmehn, and R. Waser, Z. Phys. Chem. **221**, 1469 (2007).
[24] M. Mitkova, Y. Wang, and P. Boolchand, Phys. Rev. Lett. **83**, 3848 (1999).
[25] C. P. McHardy, A. G. Fitzgerald, P. A. Moir, and M. Flynn, J. Phys. C **20**, 4055 (1987).
[26] R. Soni, M. Meier, A. Rüdiger, B. Holländer, C. Kügeler, and R. Waser, Microelectron. Eng. **86**, 1054 (2009).
[27] R. Soni, P. Meuffels, H. Kohlstedt, C. Kügeler, and R. Waser, Appl. Phys. Lett. **94**, 123503 (2009).
[28] S. Machlup, J. Appl. Phys. **25**, 341 (1954).
[29] C. E. Parman, N. E. Israeloff, and J. Kakalios, Phys. Rev. B **47**, 12578 (1993).
[30] L. M. Lust and J. Kakalios, Phys. Rev. Lett. **75**, 2192 (1995).
[31] M. B. Weissman, Rev. Mod. Phys. **60**, 537 (1988).
[32] K. S. Ralls and R. A. Buhrman, Phys. Rev. Lett. **60**, 2434 (1988).
[33] I. Zvyagin, in *Charge Transport in Disordered Solids with Application in Electronics*, edited by S. Baranovski (Wiley, London, 2006), Chap. 9.
[34] I. Chaudhuri, F. Inam, and D. A. Drabold, Phys. Rev. B **79**, 100201 (2009).
[35] D. R. Bowman and D. Stroud, Phys. Rev. B **40**, 4641 (1989).

[36]B. Kahng, G. G. Batrouni, and S. Redner, J. Phys. A **20**, L827 (1987).
[37]E. S. Machlin, *An Introduction to Aspects of Thermodynamics and Kinetics Relevant to Materials Science* (Giro, Croton-on-Hudson, New York., 1991).
[38]M. B. Weissman, Phys. Rev. Lett. **86**, 1390 (2001).
[39]E. Bychkov, Solid State Ion. **136–137**, 1111 (2000).
[40]A. Pradel, G. Taillades, C. Cramer, and M. Ribes, Solid State Ion. **105**, 139 (1998).
[41]R. T. Wakai and D. J. Van Harlingen, Appl. Phys. Lett. **49**, 593 (1986).
[42]D. Stauffer and A. Aharony, *Introduction to Percolation Theory* (Taylor and Francis, Washington, DC, 1992).
[43]S. B. Lee, S. Park, J. S. Lee, S. C. Chae, S. H. Chang, M. H. Jung, Y. Jo, B. Kahng, B. S. Kang, M. J. Lee, and T. W. Noh, Appl. Phys. Lett. **95**, 122112 (2009).
[44]M. Nardone, V. I. Kozub, I. V. Karpov, and V. G. Karpov, Phys. Rev. B **79**, 165206 (2009).